

# Avalanche upconversion in Tm:YALO<sub>3</sub>

H. Ni and S. C. Rand

Department of Electrical Engineering and Computer Science, University of Michigan, 1301 Beal Avenue, Ann Arbor, Michigan 48109-2122

Received January 16, 1991

We report the sudden appearance of upconversion fluorescence and resonant increasing absorption above a threshold intensity in Tm:YALO<sub>3</sub> at room temperature. These effects are shown to arise from nonlinear, cooperative, excited-state dynamics. Comparison with quantum theory reveals essential roles both for pairwise cross relaxation and excitation migration among Tm impurity ions.

Absorption features with thresholds in rare-earth crystals were first observed in Pr:LaCl<sub>3</sub> and Pr:LaBr<sub>3</sub> by Chivian *et al.*<sup>1</sup> in spectral regions devoid of ground-state transitions. Their experiments were a prelude to development of avalanche upconversion lasers<sup>2,3</sup> operating at shorter wavelengths than their excitation and sustained by optical pumping in regions of transparency. While empirical modeling of the nonlinear absorption<sup>4</sup> observed under avalanche conditions has supported a picture that involves cooperative energy-pooling pair processes between excited and neighboring ground-state ions, basic premises of this model have not been directly tested experimentally. Furthermore no microscopic theory has been advanced that explains observations made to date consistently.

In this Letter we present experimental results on avalanche absorption and upconversion in a new system at room temperature as well as a quantum theoretical framework for calculating system behavior. We show that when incident light is tuned away from ground-state absorption wavelengths and into resonance with an excited-state transition of Tm, nonlinear absorption and upconversion fluorescence appear above a distinct threshold intensity. We verify directly that population in the lower resonant excited state undergoes a rapid increase that may aptly be called an avalanche and cannot be explained by linear dynamics. Theoretical analysis indicates that the cooperative dynamics responsible for the avalanche involve two distinct processes, namely, near-neighbor cross relaxation and excitation migration between pairs. Collectively, these results furnish a consistent conceptual basis for a detailed understanding of avalanche upconversion and show that in selected media this phenomenon can occur at high enough temperatures to render applications practical.

Figure 1 displays both the low-intensity absorption spectrum and the excitation spectrum of induced absorption features near 649.5 nm in the biaxial host crystal YALO<sub>3</sub>. A continuous-wave, single-mode DCM ring dye laser polarized along a principal axis was tuned to the wavelength of the excited-state transition of Tm<sup>3+</sup> at 649.5 nm (Fig. 2) and focused to a spot radius of 45.0 μm in an 8-mm-thick sample. The dopant concentration was 2%.

Absorption between 640 and 660 nm was negligible at low incident intensities. However, as shown in Fig. 3, transmission in Tm:YALO<sub>3</sub> decreases sharply at a resonant wavelength of 649.5 nm above intensities of  $9.4 \times 10^2$  W/cm<sup>2</sup>. This wavelength corresponds precisely to the wavelength of the <sup>3</sup>H<sub>4</sub>(1)–<sup>1</sup>G<sub>4</sub>(1) excited-state transition of Tm.<sup>5</sup> Absorption becomes so highly nonlinear above threshold that an input beam of Gaussian profile evolves into a doughnut distribution with nearly zero transmission at beam center and relatively high transmission in the wings. At the same time strong blue upconversion fluorescence is emitted by the crystal.

We investigated the mechanism responsible for this nonlinear absorption and upconversion by first noting that efficient cross relaxation between levels <sup>3</sup>F<sub>4</sub> and <sup>3</sup>H<sub>6</sub> of Tm occurs in a wide variety of crystals doped heavily with this ion.<sup>6</sup> This process is illustrated in Fig. 2, and, since the lower level (<sup>3</sup>H<sub>4</sub>) of the induced absorption transition is the same as the intermediate state in cross relaxation, it is natural to inquire about its potential role in avalanche dynamics. To investigate excited-state dynamics, we recorded fluorescence at two wavelengths as a function of incident intensity with the laser tuned to the strongest excited-state resonance. Long-wavelength fluorescence at 1.9 μm [<sup>3</sup>H<sub>4</sub>(1)–<sup>3</sup>H<sub>6</sub>(1,2)] was detected with an InAs photodiode and used to monitor <sup>3</sup>H<sub>4</sub> excited-state population directly. Short-wavelength emission at 475.6 nm [<sup>1</sup>G<sub>4</sub>(1)–<sup>3</sup>H<sub>6</sub>(1)] was used to monitor upconversion behavior versus intensity at 649.5 nm.

Fluorescence intensity is strictly proportional to the initial-state population, irrespective of the final-state dynamics. Hence results for emission at 1.9 μm versus the incident intensity (Fig. 4) constitute a direct measurement of population in the <sup>3</sup>H<sub>4</sub> excited state. Absorption at 649.5 nm, on the other hand, reflects population differences of the <sup>3</sup>H<sub>4</sub> and <sup>1</sup>G<sub>4</sub> levels rather than of the avalanche population itself. Short-wavelength emission at 475.6 nm again samples population in the upper resonant state directly. Our results clearly show that the population itself in the <sup>3</sup>H<sub>4</sub>(1) level of Tm exhibits a dramatic increase above a relatively sharp threshold intensity. At the same time, increasing absorption

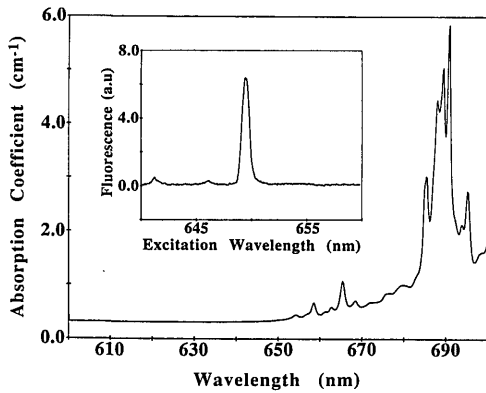


Fig. 1. Unpolarized absorption spectrum of 2% Tm:YAlO<sub>3</sub> at room temperature and low intensity. Induced absorption resonances appear between 640 and 650 nm at intensities above  $10^3$  W/cm<sup>2</sup>, as shown by the inset excitation spectrum of 475.6-nm fluorescence. In the inset, the main resonance is due to the  $^3H_4(1) \rightarrow ^1G_4(1)$  excited-state transition of Tm<sup>3+</sup>. Smaller features at 646 and 641 nm correspond to the  $^1G_4(2) \rightarrow ^3H_4(1)$  and  $^1G_4(4) \rightarrow ^3H_4(1)$  avalanche transitions, respectively.

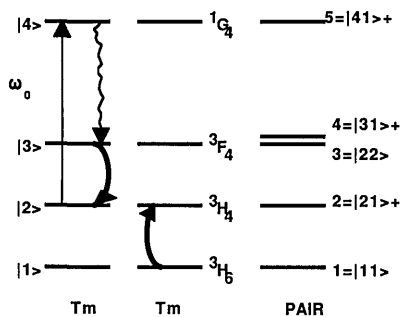


Fig. 2. Left: energy-level diagram illustrating cooperative relaxation of neighboring Tm ions. The straight arrow indicates an absorptive optical transition at frequency  $\omega_0$  followed by intraconfigurational relaxation (wiggly arrow). The curved arrows indicate the subsequent spontaneous pair process in which one  $^3F_4$  ion relaxes to  $^3H_4$  while its neighbor is promoted to the same state in a nearly resonant cooperative transition. Right: levels of the pair basis formed from uncoupled product states. States labeled + indicate that for degenerate states only the symmetric Davydov component is presumed to participate in dynamics, having nonzero matrix elements for optical transitions to ground and other + states in the presence of inversion symmetry of the pair [ $|21\rangle + = 2^{1/2}(|2\rangle|1\rangle + |1\rangle|2\rangle)$ ].

and upconversion fluorescence appear with the same threshold, in qualitative agreement with earlier observations on Pr ions.<sup>1,4</sup> Here, however, the avalanche level population is monitored directly rather than indirectly, no abrupt jumps in system parameters are observed, and room-temperature operation is achieved. Additionally, theoretical analysis of these data, which we turn to now, achieves good agreement with experiment and reveals new aspects of the avalanche upconversion process not recognized previously.

Descriptions of avalanche dynamics to date have focused on pair interactions using rate equations. However, the rate approximation provides an incomplete theory for the avalanche effect for two reasons.

First, with this approach, cooperative population decay rates (probabilities) of neighboring atoms are written in terms of uncorrelated products of occupation probabilities for individual atoms. This is contrary to the basic picture of the cooperative mechanism responsible for the avalanche in which neighboring ions make simultaneous (and therefore completely correlated) energy-conserving transitions mediated by short-range interactions.<sup>1</sup> Second, cooperative relaxation rates must dominate natural decay rates when avalanche effects are observed, so that the implicitly perturbative approach of rate equations that ignores coherences is not justified *a priori*. To include interion coherences, we started with the Liouville equation,

$$i\hbar \frac{d}{dt} \rho = [H, \rho] - i\hbar \Gamma(\rho)\rho, \quad (1)$$

where  $H = H_0 + H_{\text{int}} + V$  is the Hamiltonian,  $H_{\text{int}}$  is the interion coupling (multipole or exchange interac-

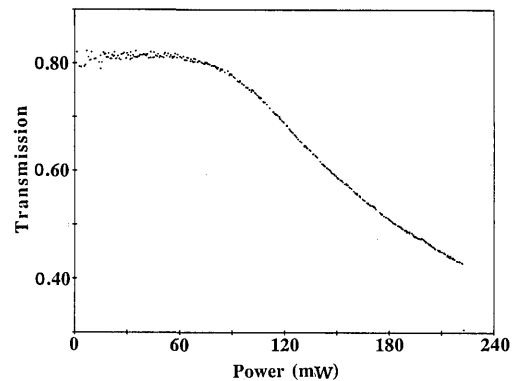


Fig. 3. Total Gaussian beam transmission through 2% Tm:YAlO<sub>3</sub> at 649.5 nm as a function of intensity ( $I = 293$  K).

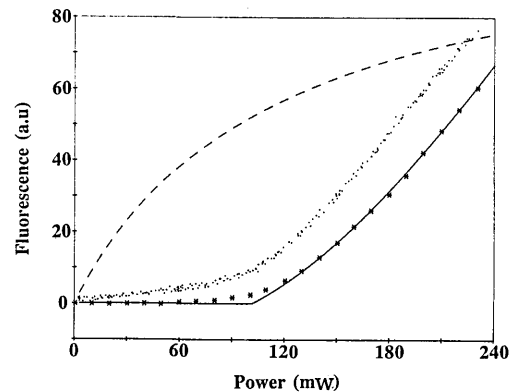


Fig. 4. Theoretical and experimental excited-state populations in 2% Tm:YAlO<sub>3</sub> excited with monochromatic light at 649.5 nm. Asterisk and dotted experimental traces: upconversion and infrared fluorescence at 475.6 nm and 1.9  $\mu$ m, respectively. Dashed curve: calculation of  $^1G_4$  population in isolated pairs ( $\alpha = 0$ ), indicative of increasing  $^3H_4$  population (magnified by  $2 \times 10^{11}$  to be visible on the scale of other calculations). Solid curve: numerical  $^1G_4$  results combining intrapair relaxation with energy migration between distant pairs (best fit  $\alpha = 2.0 \times 10^5$  s<sup>-1</sup>). The fixed parameters are  $\lambda = 2.8 \times 10^{-10}$  s<sup>-1</sup>,  $|H_{34}|^2/\hbar^2\Gamma_{34} = 10^3$  s<sup>-1</sup>,  $\gamma_{31} = \gamma_{42} = \gamma_{43} = \gamma_{51} = \gamma_{52} = \gamma_{53} = 0$ ,  $\gamma_3 = \gamma_{32} = 107$  s<sup>-1</sup>,  $\gamma_4 = \gamma_{41} = 780$  s<sup>-1</sup>, and  $\gamma_5 = \gamma_{54} = 3.6 \times 10^3$  s<sup>-1</sup>.

tions), and  $V$  describes the light-matter interaction. The relaxation rate given by phenomenological damping term  $-i\hbar\Gamma(\rho)\rho$  in our semiclassical approach is linear in atomic density for intrapair dynamics in a pair basis of states but bilinear for relaxation between uncorrelated pairs.  $\Gamma$  depends on  $\rho$  since decay can occur not only internally but also by random hopping of excitation to a distant pair with a rate dependent on pair populations at the origin and destination. Equation (1) in the uncoupled pair basis of Fig. 2 yields the following equations for populations in pair levels coupled by the optical field:

$$\begin{aligned} \frac{d}{dt}\rho_{22} = & (V_{25}\rho_{52} - \rho_{25}V_{52})/i\hbar - \gamma_{21}\rho_{22} + \lambda(\rho_{11} - \rho_{22}) \\ & + \gamma_{32}\rho_{33} + \gamma_{42}\rho_{44} + \gamma_{52}\rho_{55} + 2\alpha\rho_{11}\rho_{33} - 2\alpha\rho_{22}^2, \end{aligned} \quad (2)$$

$$\frac{d}{dt}\rho_{55} = (V_{52}\rho_{25} - \rho_{52}V_{25})/i\hbar - \gamma_5\rho_{55}. \quad (3)$$

These equations must be solved self-consistently with those for populations in other levels, as well as for optical and interatomic coherences,

$$\frac{d}{dt}\rho_{25} = i\omega_0\rho_{25} + V_{25}(\rho_{55} - \rho_{22})/i\hbar - \Gamma_{25}\rho_{25}, \quad (4)$$

$$\begin{aligned} \frac{d}{dt}\rho_{34} = & \rho_{34}(H_{33} - H_{44})/i\hbar \\ & + H_{34}(\rho_{44} - \rho_{33})/i\hbar - \Gamma_{34}\rho_{34}, \end{aligned} \quad (5)$$

These equations reduce to rate equations when the interatomic coherence is zero ( $H_{34} = \langle 3|H_{\text{int}}|4\rangle = 0$ ).  $\gamma_{ij}$  is the decay rate from level  $i$  to  $j$ ,  $\gamma_k$  is the total rate from level  $k$ , and  $\rho_{kl}$  is the density-matrix element between pair levels  $k$  and  $l$ .  $\Gamma_{ij}$  is the rate of relaxation of coherence between levels  $i$  and  $j$ , and  $\lambda$  is a thermal pumping rate, assumed to be effective solely in populating the first excited pair state.  $\alpha$  is the rate of resonant energy migration between distant pairs ( $\rho$  is dimensionless).

Coefficient  $\alpha$  accompanies nonlinear terms that describe dynamics between uncorrelated pairs. For example, the term  $+2\alpha\rho_{11}\rho_{33}$  in Eq. (2) describes the relaxation of two pairs initially in pair states 3 and 1. Energy exchange yields two pairs in state 2 at a rate  $\alpha$ . Linearized theory ( $\alpha = 0$ ) describes coherent dynamics within isolated pairs and predicts a minute amount of increasing absorption, as indicated by the dashed curve in Fig. 4. However, it does not reproduce other experimental observables such as the threshold of avalanche absorption, its qualitative dependence on intensity, or its magnitude. Hence cooperative decay within isolated pairs is by itself inadequate to account for avalanche behavior.

Individual pairs undergoing cross relaxation can increase the population of the avalanche level but can at most double the weak initial absorption due to overlapping ground-state transitions or thermally excited Tm ions in the first excited state. Hence isolated pairs can initiate minor increases but cannot account for strong induced absorption. Correlated dynamics within isolated pairs is therefore

an essential mechanism by which ions reach an ordinarily empty excited state, but a mechanism must also exist for rapid excitation migration involving more ions to achieve substantial increases in absorption.

Evidence for this is presented in Fig. 4, in which the solid curve shows the result when  $\alpha$  is taken to be nonzero. This introduces resonant energy migration (random hopping) between state-3 pairs and distant ground-state neighbors, which constitute a reservoir of excitable atoms. For simplicity, we disregard the detailed nature and distance dependence of the migration process ( $\alpha = \text{constant}$ ), retaining only a bilinear dependence on occupation probabilities of pairs at the origin and destination in the corresponding relaxation rate.

Good agreement with experiment is obtained with the full theory, which permits a majority of impurity ions to participate in cooperative dynamics through combined intrapair and interpair relaxation. The small discrepancy in Fig. 4 between the solid theoretical curve and data near threshold is attributed to nonuniformity of interaction across the Gaussian beam. Agreement is therefore only obtained when the internal dynamics of near-neighbor atomic interactions is followed by energy transfer to more distant Tm ions, with a transfer rate independent of the identity of the initial pair by virtue of randomness in the migration process. Clearly, slow near-neighbor dynamics yield increasing absorption, whereas fast migration yields threshold behavior and immensely magnifies the excited-state absorption.

In summary, we have identified two important aspects of avalanche dynamics, describable by a single set of equations. First, light that is not resonant with any ground-state absorption promotes ions to excited states by activating short-range interactions between one excited ion and a near neighbor in the ground state, which generates increased absorption. Second, energy migration multiplies the effectiveness of the cooperative dynamics, which introduces a characteristic absorption threshold. In 2% Tm:YALO, avalanche absorption and upconversion are observed at room temperature and are well described by density-matrix theory.

This research was sponsored by Air Force Office of Scientific Research contract F49620-88-C-0079.

## References

1. J. Chivian, W. Case, and D. Eden, *Appl. Phys. Lett.* **35**, 124 (1979).
2. M. Koch, A. Kueny, and W. Case, *Appl. Phys. Lett.* **56**, 1083 (1990).
3. R. M. MacFarlane, R. Wannemacher, T. Hebert, and W. Lentz, in *Digest of Conference on Lasers and Electro-Optics* (Optical Society of America, Washington, D.C., 1990), paper CWF1 and references therein.
4. A. Kueny, W. Case, and M. Koch, *J. Opt. Soc. Am. B* **6**, 639 (1989).
5. L. M. Hobrock, Ph.D. dissertation (University of Southern California, Los Angeles, Calif., 1972). We use the spectroscopic designations of Hobrock throughout.
6. R. Stoneman and L. Esterowitz, *Opt. Lett.* **15**, 486 (1990).